

## The metal–insulator transition in $V_2O_3(0001)$ thin films: surface termination effects

This article has been downloaded from IOPscience. Please scroll down to see the full text article.

2005 J. Phys.: Condens. Matter 17 4035

(<http://iopscience.iop.org/0953-8984/17/26/004>)

View [the table of contents for this issue](#), or go to the [journal homepage](#) for more

Download details:

IP Address: 129.252.86.83

The article was downloaded on 28/05/2010 at 05:12

Please note that [terms and conditions apply](#).

# The metal–insulator transition in $V_2O_3(0001)$ thin films: surface termination effects

F Pfuner, J Schoiswohl, M Sock, S Surnev, M G Ramsey and F P Netzer

Institute of Physics, Surface and Interface Physics, Karl-Franzens University Graz,  
A-8010 GRAZ, Austria

Received 18 March 2005

Published 17 June 2005

Online at [stacks.iop.org/JPhysCM/17/4035](http://stacks.iop.org/JPhysCM/17/4035)

## Abstract

Epitaxially grown  $V_2O_3(0001)$  thin films have been prepared with different surface terminations, as evidenced by atomically resolved scanning tunnelling microscopy and high-resolution electron energy loss spectroscopy (HREELS) phonon spectra. The spectral changes observed in valence band photoemission spectra and HREELS on cooling the  $V_2O_3$  samples from 300 to 100 K have been associated with the metal–insulator transition (MIT) in the bulk of the  $V_2O_3$  film. The reconstructed surface regions *per se* do not display the MIT, but affect the MIT signature observed with surface sensitive techniques, depending on the thickness of the reconstructions. Whereas the thermodynamically stable  $(1 \times 1)$  vanadyl  $V=O$  surface termination allows the observation in photoemission and HREELS of a clear signature of the MIT, the latter is screened on a  $(\sqrt{3} \times \sqrt{3})R30^\circ$  surface formed by  $V=O$  defect structures. Doping of the  $(\sqrt{3} \times \sqrt{3})R30^\circ$  surface with small amounts of adsorbed water restores reversibly the MIT spectral fingerprints. These observations are discussed in terms of the different geometrical and electronic structures of the different surface terminations.

(Some figures in this article are in colour only in the electronic version)

## 1. Introduction

The metal–insulator transition (MIT) in pure and doped vanadium sesquioxide [1, 2], which occurs as a function of temperature, pressure and doping level, is of both experimental and theoretical interest and even almost 60 years after its discovery it is still an active area of research. The complex phase diagram of  $V_2O_3$  contains paramagnetic metal, paramagnetic insulator, and antiferromagnetic insulator regions, and phase transitions may be induced by changes in temperature, chemical composition, or pressure. In pure  $V_2O_3$  the transition from the paramagnetic metallic to the antiferromagnetic insulating phase occurs at  $T_C \approx 150$ – $160$  K and it involves a structural transformation from a trigonal corundum structure at  $T > T_C$  to a monoclinic structure at  $T < T_C$ . The MIT in  $V_2O_3$  has been generally considered to be a

classical example of a Mott–Hubbard transition, but recent experimental results showing the importance of electron lattice interaction and orbital degeneracy [3, 4] could not be explained within the single-band Hubbard model. This has prompted an intense theoretical discussion on this compound, as summarized in a recent contribution by Di Matteo *et al* [5]. The spectral signature of the strongly interacting system is reflected in principle in photoemission spectra, where a distinctive quasiparticle peak at the Fermi energy in the metallic phase decreases with increasing on-site Coulomb repulsion  $U$  and vanishes at a critical value of the ratio of  $U$  to the bandwidth  $B$ , which marks the MIT [6]. However, photoemission is a surface sensitive technique and in particular at low photon energies surface effects may dominate over bulk effects, yielding spectra not characteristic of the bulk electronic structure [7]. The latter may be significant because the surface region of the metallic phase may be more strongly correlated than the bulk [8], because the lower coordination on the surface reduces the bandwidth relative to the bulk, thus reducing the screening of  $U$  and increasing the  $U/B$  ratio at the surface.

A drawback of most experimental studies reported on  $V_2O_3$  single-crystal samples is that surface effects have been mostly neglected and that the sample surfaces were rough and crystallographically ill defined due to the sample cleaning techniques employed, such as e.g. scraping with a hard tool. Moreover, the surface structures have not been characterized at the atomic level. This may have important consequences, since surface reconstructions may cause severe rearrangements of surface atoms with concomitant modifications of the surface electronic structure as compared to the bulk. In this paper we will show that this is indeed the case for  $V_2O_3$ .

Recently, Preisinger *et al* [9] have prepared single-crystal  $V_2O_3(0001)$  surfaces in two modifications by annealing in vacuum at  $750^\circ\text{C}$  and by Ar ion sputtering followed by annealing. Scanning tunnelling microscopy has been applied to these surfaces, but the surface structures could not be unambiguously resolved. The annealed surface was apparently reconstructed, whereas the sputtered surface showed bulk-like unit cell dimensions with a large number of surface defects. The reported He I photoemission spectra were different for the two surface modifications, with a different spectral weight of the quasiparticle peak at the Fermi energy [9]. Epitaxial thin films of  $V_2O_3$  have been grown on sapphire substrates by several groups [10–12] and the influence of strain, introduced in the films due to interfacial lattice mismatch, on the electrical behaviour has been addressed. Schuler *et al* [10] found a different behaviour of the  $V_2O_3$  phase transitions depending on the preparation conditions of the films, and Luo *et al* [11] reported that the MIT depends on the film thickness, with the MIT suppressed for ultrathin films. However, the electrical measurements in the latter case have been performed *ex situ* [11], and neither stoichiometry nor morphology of the films were known. Conversely, Sass *et al* [12] found bulk-like properties with respect to the MIT in their  $V_2O_3$  films, which were grown on sapphire with a  $(1\bar{1}20)$  surface orientation.

In recent work we have grown epitaxial  $V_2O_3$  nanolayers, i.e. ultrathin films of thickness 5–8 nm (20–30 monolayers), on metal single-crystal substrates under very well controlled conditions, and have characterized the surfaces experimentally at the atomic level by low-energy electron diffraction (LEED), high-resolution scanning tunnelling microscopy (STM), photoelectron spectroscopy with use of synchrotron radiation, and high-resolution electron energy loss spectroscopy (HREELS) [13]. By combining the experimental results with *ab initio* density functional theory [14] the stable surface terminations of  $V_2O_3$  have been investigated: it was found that the possible ideal bulk terminations are unrealistic and that novel surface reconstructions have to be considered. In the present paper we report photoemission and HREELS phonon spectra recorded at room temperature and at 100 K of differently terminated  $V_2O_3(0001)$  thin-film surfaces and investigate their relation to the MIT of  $V_2O_3$ . The influence of the surface termination and of adsorbates on the MIT will be addressed.

In section 2 of this paper the atomic structures of the different surface terminations of  $V_2O_3(0001)$  are introduced, and in section 3 the experimental procedures for obtaining these surfaces are described. Section 4 presents the results of this study and their discussion, and a brief conclusion, section 5, terminates the paper.

## 2. Surface terminations of $V_2O_3(0001)$

Vanadium sesquioxide at room temperature in its metallic form has a rhombohedral corundum structure which may be represented perpendicular to the  $[0001]$  direction by a  $\cdots-V_2O_3V_2O_3-\cdots$  stacking sequence of planes. The oxygen atoms form hexagonal planes with three oxygen atoms per layer in the hexagonal unit cell, whereas the vanadium atoms are located in a slightly buckled bilayer. Three possible ideal bulk terminations can be envisioned for the  $(0001)$  surface plane: (i) oxygen termination by an  $O_3$  layer; (ii) vanadium termination by a  $V_2$  bilayer; and (iii) vanadium termination by a V single layer, corresponding to a  $\cdots-V_2O_3-V$  stacking sequence at the surface. Kresse *et al* [14] have investigated the stability of these bulk terminated surfaces by *ab initio* DFT theory and found that the  $V_2$  bilayer terminated surface is highly unstable and that the singly V terminated surface is stable only at very low chemical potentials of oxygen, i.e. at very reducing conditions [13]. The oxygen terminated surface is stable under an oxygen-rich ambient. This thermodynamically stable  $O_3$  termination is not simply a continuation of the corundum bulk structure, but the corresponding surface region relaxes in such a way that a V atom from the second  $V_2$  bilayer pops up into the first  $V_2$  bilayer below the top  $O_3$  layer. The result is a  $-V_2O_3-V-O_3V_3O_3$  stacking sequence at the surface; it may also be regarded as an  $O_3V_3O_3$  trilayer structure with a formal  $VO_2$  stoichiometry on top of the non-polar singly V terminated bulk termination.

However, over a wide range of oxygen chemical potentials the most stable termination of the  $V_2O_3(0001)$  surface in thermodynamic equilibrium with the bulk is a surface terminated with vanadyl  $V=O$  groups. It forms a  $(1 \times 1)$  surface structure with respect to the bulk unit cell and may be regarded as the ideal single-metal terminated surface with one additional oxygen atom bonded on top of each outermost V atom. Alternatively, this vanadyl  $(1 \times 1)$  surface may be envisaged as an  $O_3$  terminated surface with one  $V=O$  group per unit cell adsorbed in the threefold hollow sites of the oxygen layer (see the model in figure 1(c)). Note that the  $V=O$  units are not contained in the regular  $V_2O_3$  corundum structure, but that they are structural building blocks of the higher  $V_2O_5$  oxide.

The theoretically proposed stable vanadyl termination of the  $V_2O_3(0001)$  surface is fully confirmed by the experimental results. Figure 1 shows STM (a) and LEED (b) pictures of the  $(1 \times 1)$  vanadyl surface of a ten-monolayer (8 nm) thick film of  $V_2O_3$  grown epitaxially on a Rh(111) substrate. The main frame of figure 1(a) shows large flat terraces of the  $V_2O_3(0001)$  surface and the sharp LEED pattern (figure 1(b)) is characteristic of the good long-range order. The inset of figure 1(a) is a high-resolution STM image displaying atomic resolution of the vanadyl groups, which are imaged as the bright maxima [13] forming the indicated unit cell with the correct bulk  $V_2O_3$  dimensions. The  $V=O$   $(1 \times 1)$  surface is illustrated in the structure model of figure 1(c). The most decisive evidence for the vanadyl termination has been found in the HREELS phonon spectrum of the  $V_2O_3(0001)$  surface, as displayed in figure 2(a). The spectrum contains prominent electron loss peaks at 47, 78, and 129 meV, a weak shoulder at 92 meV, and a weak structure at  $\sim 156$  meV. Whereas the losses at  $<100$  meV may be associated with the phonons of the  $V_2O_3$  lattice structure (see below), the peak at 129 meV is too high in energy to be associated with singly bonded oxygen species. It is the signature of a vanadium–oxygen double bond, i.e. its stretching frequency, as has been found in the vanadyl  $V=O$  species containing  $V_2O_5$  [15].

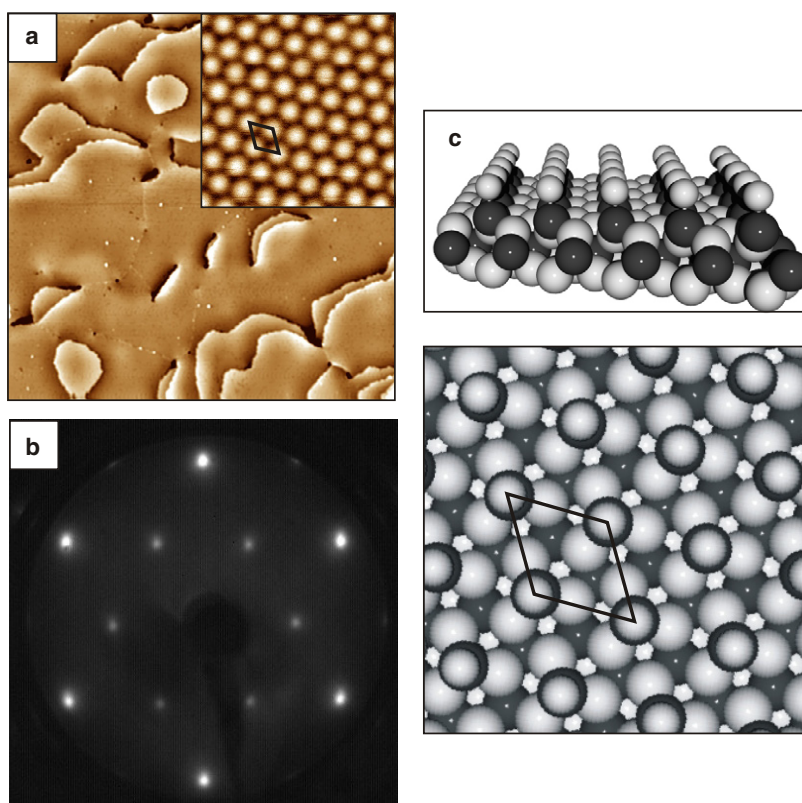


**Figure 1.** STM (a) and LEED (b) images of the vanadyl terminated  $V_2O_3(0001)$   $V=O$  ( $1 \times 1$ ) surface. (a)  $200 \text{ nm} \times 200 \text{ nm}$ ; tunnelling conditions 2.0 V, 0.1 nA; (b) electron energy  $E_p = 55 \text{ eV}$ . (c) A model of the surface in top and side view (vanadium, dark spheres; oxygen, bright spheres). The inset of (a) shows an atomically resolved STM image, with a unit cell indicated ( $4 \text{ nm} \times 4 \text{ nm}$ , 0.2 V, 0.1 nA).

The dipole active phonons of the  $V=O$  ( $1 \times 1$ )  $V_2O_3(0001)$  surface have been calculated by Kresse *et al* [14]. Only two bulk phonon modes at 46.2 and 63.3 meV were calculated to have significant dipole intensity with contributions parallel to the  $c$ -axis (i.e. orthogonal to the hexagonal planes), but two intense surface modes at 82 and 135 meV have been predicted. Whereas the latter is the above mentioned vanadyl stretching mode, the former originates from the three oxygen atoms (in the  $O_3$  layer) below the  $V=O$  group, which vibrate parallel to their bond to the vanadyl group, i.e. essentially perpendicular to the surface.

Under oxidizing conditions (see below) the  $V=O$  ( $1 \times 1$ )  $V_2O_3(0001)$  surface may be transformed into an O-rich  $(\sqrt{3} \times \sqrt{3})R30^\circ$  surface [13, 14]. Figure 3 shows STM (a) and LEED (b) images together with a model (c) of this surface. The  $(\sqrt{3} \times \sqrt{3})R30^\circ$  structure may be formed by the removal of one or two vanadyl groups per  $\sqrt{3}$  unit cell, resulting in  $-V_2O_3-(V=O)_{0.66}$  or  $-V_2O_3-(V=O)_{0.33}$  stacking sequences, respectively. The corresponding unit cells are indicated in the model of figure 3(c). Since the removal of each  $V=O$  group exposes three oxygen atoms of the underlying  $O_3$  plane, the resulting surface becomes more oxygen rich. The DFT calculations indicate [14] that the removal of  $V=O$  groups produces  $(\sqrt{3} \times \sqrt{3})R30^\circ$  surfaces that are stable in the  $V_2O_3$  surface phase diagram. The calculations also indicate that the local creation of an  $O_3$  termination at the  $(\sqrt{3} \times \sqrt{3})R30^\circ$  surfaces induces

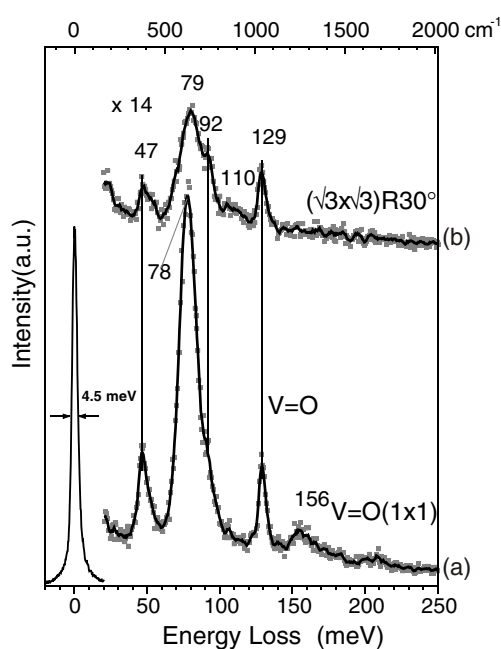


**Figure 2.** HREELS spectra of the  $V_2O_3(0001)(1 \times 1)$  (a) and  $(\sqrt{3} \times \sqrt{3})R30^\circ$  (b) surfaces recorded at 300 K.

a local relaxation of the surface in the same manner as on the extended oxygen  $O_3$  terminated surface: a V atom of the second bilayer pops up into the first bilayer, creating locally an  $-O_3V_3O_3$  trilayer structure below the  $(\sqrt{3} \times \sqrt{3})R30^\circ$  vanadyl layer. The detailed inspection of high-resolution STM images reveals that the regions of the  $(\sqrt{3} \times \sqrt{3})R30^\circ$  structure with one or two V=O groups per unit cell (i.e. two-thirds or one-third of the vanadyl groups of the  $(1 \times 1)$  structure removed) are roughly equally distributed over the surface [13].

Figure 2(b) displays an HREELS spectrum of the  $(\sqrt{3} \times \sqrt{3})R30^\circ$   $V_2O_3(0001)$  surface. In comparison to the loss spectrum of the  $(1 \times 1)$  surface (figure 2(a)) the intensities of all losses are somewhat reduced on the  $(\sqrt{3} \times \sqrt{3})R30^\circ$  surface and a weak structure is visible at  $\sim 110$  meV. The overall similarity of the loss spectrum of the  $(\sqrt{3} \times \sqrt{3})R30^\circ$  surface to the one from the  $(1 \times 1)$  surface is due to the fact that there are still V=O groups present at the  $(\sqrt{3} \times \sqrt{3})R30^\circ$  surface, albeit at lower concentration, and that the  $O_3$  oxygen termination has similar vibrational modes at  $\sim 80$  meV [14]. Due to dipole–dipole interaction effects the HREELS spectra do not reflect the differences in the concentration of V=O species between the  $(1 \times 1)$  and  $(\sqrt{3} \times \sqrt{3})R30^\circ$  surfaces in a quantitative way. We note parenthetically, however, that the reduction of the concentration of vanadyls on the  $(\sqrt{3} \times \sqrt{3})R30^\circ$  surface is clearly shown up in the V 2p core level photoemission spectra as reported previously [13].

### 3. Experimental procedures

Thin films of  $V_2O_3$  have been prepared by reactive evaporation of vanadium metal in oxygen atmosphere on a clean Rh(111) substrate surface. Typical evaporation conditions were  $p_{O_2} = 2 \times 10^{-7}$  mbar  $O_2$ , substrate temperature  $250^\circ C$ , evaporation rate  $2$  monolayer  $min^{-1}$  (one monolayer of V is defined by the density of surface atoms on the Rh(111) surface).

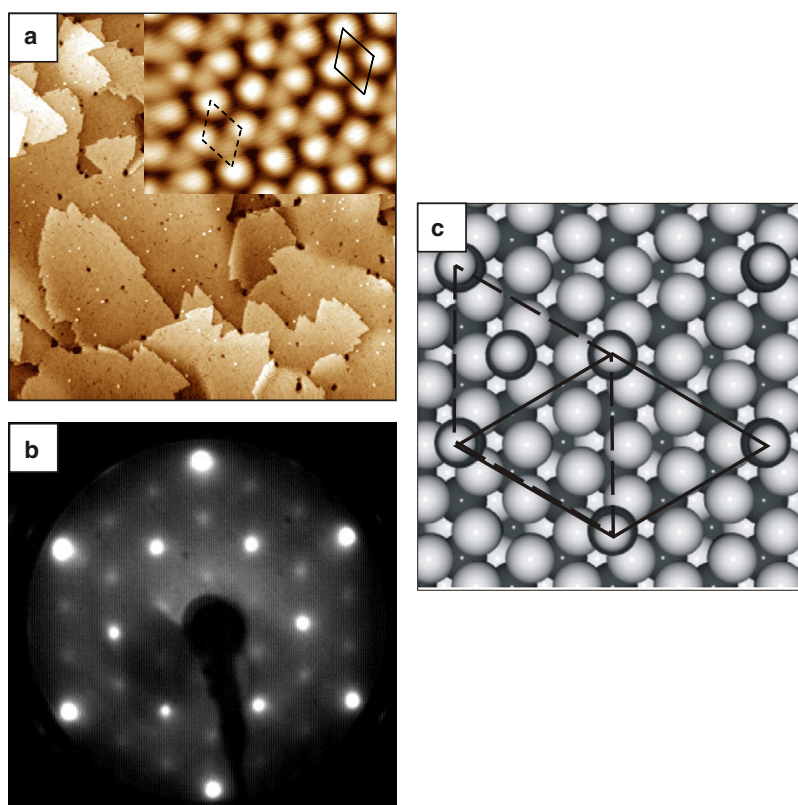


**Figure 3.** STM (a) and LEED (b) images of the  $(\sqrt{3} \times \sqrt{3})R30^\circ$  surface. (a)  $200 \text{ nm} \times 200 \text{ nm}$ ; tunnelling conditions  $2.0 \text{ V}$ ,  $0.1 \text{ nA}$ ; (b) electron energy  $E_p = 60 \text{ eV}$ . Panel (c) displays a model of the surface, with unit cells containing one (dashed) or two (solid) missing vanadyl groups indicated. The inset of (a) shows an atomically resolved STM image ( $4.5 \text{ nm} \times 3 \text{ nm}$ ,  $2.0 \text{ V}$ ,  $0.1 \text{ nA}$ ), where the two unit cells corresponding to those in (c) are marked on the picture.

Subsequent annealing in vacuum at  $600^\circ\text{C}$  for 10 min resulted in flat oxide films with excellent long-range order oriented with the  $\text{V}_2\text{O}_3(0001)$  basal plane parallel to the  $\text{Rh}(111)$  surface. The  $\text{V}_2\text{O}_3$  stoichiometry of the vanadium oxide films has been checked in photoemission by their  $\text{V } 2p_{3/2}$  core level binding energy of  $515.6 \text{ eV}$ . As discussed above and shown in figure 1 the surfaces of the  $\text{V}_2\text{O}_3$  films exhibit a  $(1 \times 1)$  structure and are terminated by vanadyl groups. Exposing the vanadyl terminated  $(1 \times 1)$  surface to oxygen ( $5 \times 10^{-6} \text{ mbar}$ ) at  $500^\circ\text{C}$  leads to the formation of a well ordered  $(\sqrt{3} \times \sqrt{3})R30^\circ$  surface (figure 3). The vanadyl groups, which have been removed from the  $\sqrt{3}$  unit cells in the process of the oxidation of the  $(1 \times 1)$  surface, have presumably migrated to the step edges as suggested by the appearance of ragged step edges and the increase of surface roughness during the oxidation (compare figures 1(a) and 2(a)). The  $\text{V}_2\text{O}_3$  films employed in this study were  $\sim 15$ – $20$  oxide layers thick, corresponding to film thicknesses of the order of  $12$ – $16 \text{ nm}$ .

The HREELS experiments have been performed in an ErEELS 31 spectrometer with a system pressure background of  $< 1 \times 10^{-10} \text{ mbar}$ , as described elsewhere [16]. HREELS spectra were taken with a primary energy of  $5.5 \text{ eV}$  in specular reflection geometry ( $60^\circ$  incidence angle w.r.t. the surface normal) with a typical resolution of  $\sim 4.5 \text{ meV}$  as measured at the FWHM of the reflected primary peak. The HREELS spectra are displayed as normalized

to the elastic peak intensity. The photoemission measurements have been carried out with He I radiation ( $h\nu = 21.2$  eV) in the laboratory in Graz and with use of synchrotron radiation at beamline I311 in the Swedish synchrotron radiation laboratory MAX-lab in Lund. In both systems photoemission spectra were recorded with a Scienta SES 200 hemispherical electron energy analyser, at background pressures  $\leq 1 \times 10^{-10}$  mbar. The He I spectra were taken with an energy resolution of 0.1 eV, whereas the synchrotron radiation spectra with  $h\nu = 517$  and 110 eV were recorded with energy resolutions of  $\sim 0.25$  and  $\sim 0.06$  eV, respectively. The samples were mounted on coolable (100 K) and heatable (1300 K) sample manipulators in all spectrometer systems.

#### 4. Results and discussion

##### *The $V_2O_3(0001)(1 \times 1)$ $V=O$ terminated surface*

Photoemission spectra of the V 3d band in the vicinity of the Fermi level of the vanadyl terminated  $V_2O_3(0001)$  surface recorded at 300 and 100 K with different photon energies are collected in figure 4. The spectra have been taken in different experimental geometries, in normal emission (NE,  $\Theta = 0^\circ$ ; figures 4(a) and (b)), which emphasises the contribution of bulk-type layers below the surface, and in grazing emission (GE,  $\Theta = 70^\circ$ ; figures 4(c) and (d)), which enhances the contribution of the surface layers. Note that the HeI spectra have been recorded at normal emission (figure 4(a)) and the  $h\nu = 517$  eV spectra at grazing emission (figure 4(d)), but that the  $h\nu = 110$  eV spectra (figures 4(b) and (c)) have been measured at both normal and grazing emission. At all photon energies there is a clear difference of the spectral profiles between the room-temperature and the low-temperature samples, with a shift of the spectral weight away from the Fermi level to higher binding energy when cooling from 300 to 100 K. This effect is more pronounced at normal emission than at grazing emission (see  $h\nu = 110$  eV spectra, figures 4(b) and (c), but the grazing emission  $h\nu = 517$  eV spectra (figure 4(d)) still show this shift of the leading edge of the V 3d structure to higher binding energy. We take these shifts and the disappearance of intensity at  $E_F$  as an indication of the metal–insulator transition occurring in the thin  $V_2O_3$  films.

However, in all spectra of figure 4 the quasiparticle peak at the Fermi energy [6] is very weak. It has to be realized in this context that the probing depth of the photoemitted electrons is low in all the experiments presented here and that the contribution of the surface layers to the spectra is dominant. The reduced coordination of atoms at the surface may lead to an increased correlation of electrons, which in turn quenches the intensity of the quasiparticle peak in the photoemission spectra [17]. In addition, however, there is an extrinsic effect which is superimposed and probably dominating the intrinsic surface effect: the outermost surface layer of  $V_2O_3$  in thermodynamic equilibrium with the bulk is not a plane of the bulk crystal structure, but it consists of vanadyl species arranged in a hexagonal array with the (0001) bulk lattice constant (see section 2). This surface layer can be expected to have a very different electronic structure than surface layers with possible bulk terminations.

Kresse *et al* have calculated the electronic local density of states of various surface terminations of  $V_2O_3$  [14]. At the surface the density of states is profoundly changed with respect to the bulk, with marked differences between the different terminations. On the vanadyl terminated surface the V atom possesses a tetrahedral oxygen coordination as opposed to an octahedral coordination of V atoms in the bulk. This implies for the conduction band V 3d states that two  $e_g$  states are located around the Fermi level and that the triply degenerate  $t_{2g}$  states are located well above. In the bulk with an octahedral-type coordination (note that the symmetry is not perfectly rhombohedral) the three V  $t_{2g}$  orbitals dominate around the Fermi



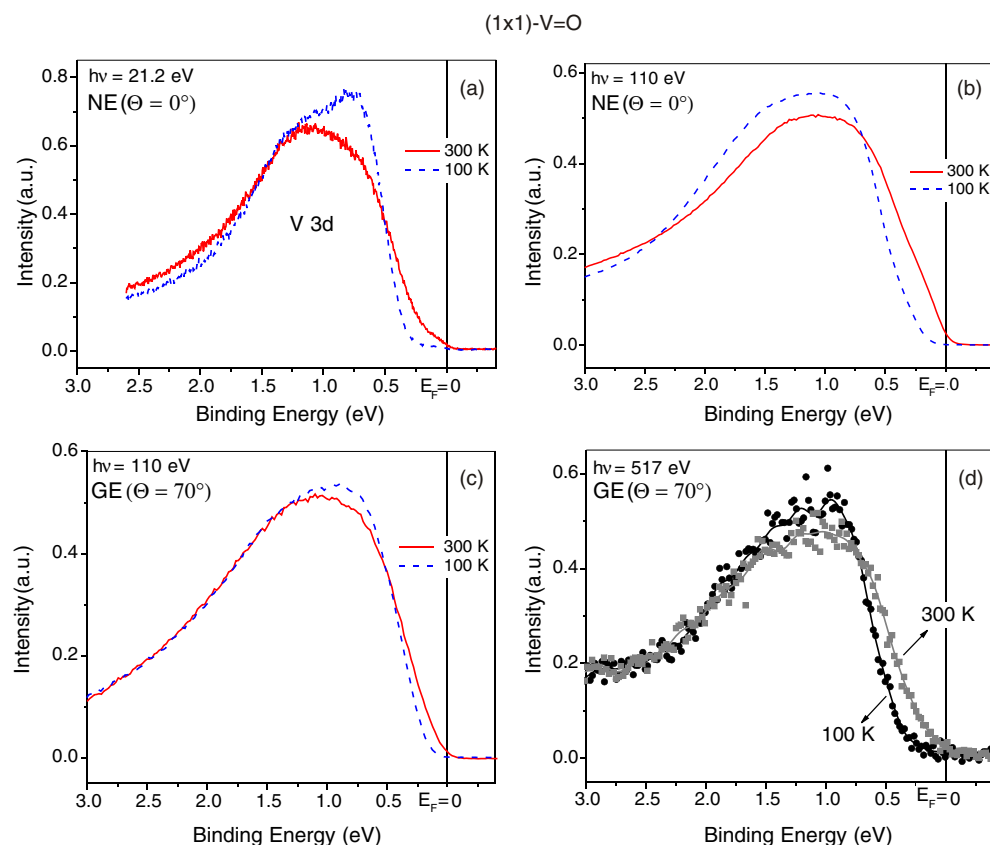


**Figure 4.** V 3d valence band photoemission spectra recorded at 300 and 100 K with the indicated photon energies. The spectra in (a) and (b) have been taken in normal emission geometry, whereas the spectra in (c) and (d) have been taken in grazing emission ( $70^\circ$  with respect to the surface normal). The spectra have been normalized to display an equal area in the range from  $E_F$  to 3 eV binding energy after subtraction of a Shirley-type background.

level and the  $e_g$  states are located well above. The number of conduction band d electrons is reduced to  $\sim 0.4$  in the vanadyl group, whereas it is close to 2 per V atom in bulk  $V_2O_3$ . It is therefore very unlikely that the vanadyl surface layer with its different geometry and electronic structure can support the MIT of  $V_2O_3$ . However, what we see in the experiments seems to be the *manifestation of the MIT* in the bulk of the  $V_2O_3$  film as *communicated through the vanadyl surface layer*.

The HREELS results of figure 5 confirm this conjecture. In figure 5 HREELS spectra of the V=O ( $1 \times 1$ ) surface as recorded at 300 and 100 K are compared. The phonon spectra change significantly upon cooling: the structure at 78 meV shifts to 83 meV and increases remarkably in intensity (by a factor of two); a new loss peak at 66 meV appears, whereas the losses at 47 and 129 meV remain largely unchanged. The 166 meV feature is the double loss of the 83 meV phonon, which is prominent in the low-temperature spectrum because of the large intensity of the latter. Similar observations in HREELS upon cooling of  $V_2O_3$  thin-film samples have been reported by Guo *et al* [18] and Dupuis *et al* [19]; the observed modifications thus provide a qualitative fingerprint of the MIT. Interestingly, the most pronounced effect of the MIT in the HREELS spectra concerns the loss feature at 78 meV, which originates from

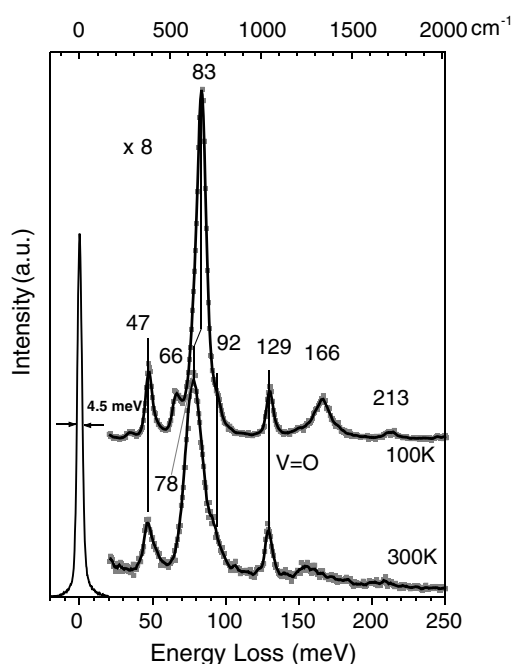
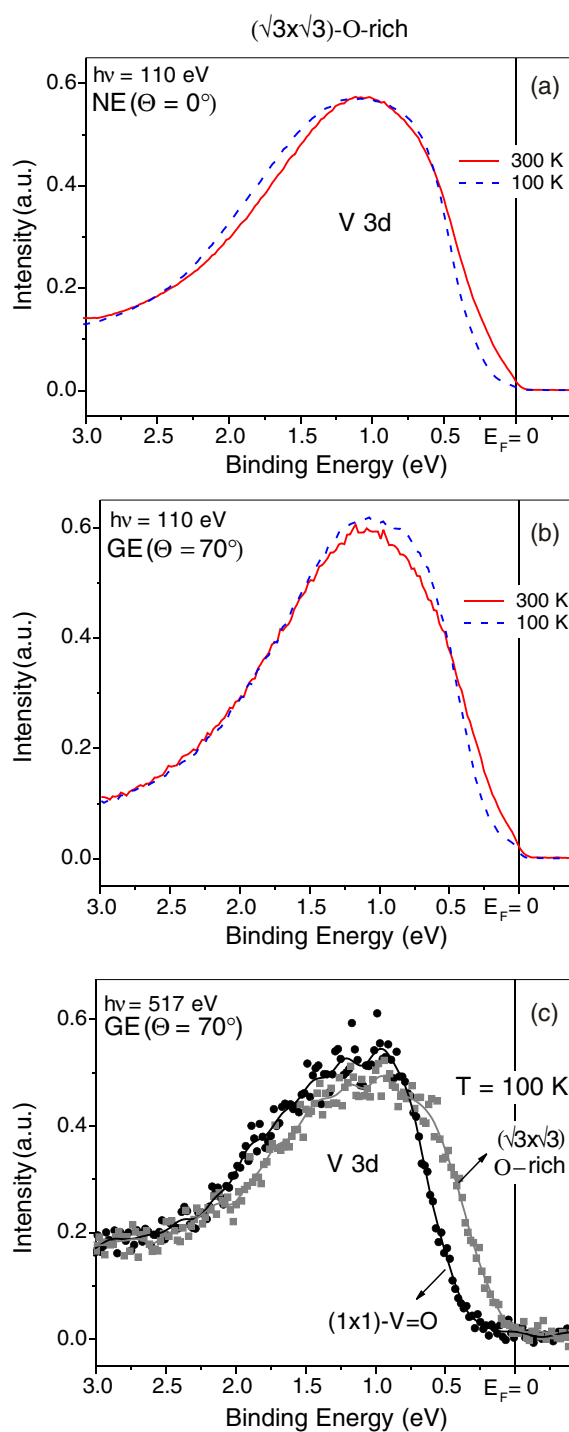


Figure 5. HREELS spectra of the  $V_2O_3(0001)$   $V=O(1 \times 1)$  surface recorded at 300 and 100 K.

a surface-related vibration, namely the vibration perpendicular to the surface of the three oxygen atoms below the vanadyl group, located in the oxygen  $O_3$  layer [14]. This  $O_3$  layer is the first bulk-like layer of the  $-V_2O_3V_2O_3-V=O$  stacking sequence on the  $V=O(1 \times 1)$  surface and it appears to reflect the structural changes of the MIT in the bulk. In contrast, the bulk phonon at 47 meV [14] appears to be uninfluenced. We conjecture that the new loss peak at 66 meV in the 100 K spectrum is also a bulk vibration [14], which is hidden in the 300 K spectrum by the loss at 78 meV. Alternatively, a splitting of the phonon at 78 meV (into 66 and 83 meV components) would be compatible with the structural symmetry reduction that occurs in going from the rhombohedral metallic phase to the insulating monoclinic phase. The lack of changes in the  $V=O$  stretching vibration at 129 meV indicates that the vanadyl surface layer is not directly influenced by the MIT.

#### *The $V_2O_3(0001)(\sqrt{3} \times \sqrt{3})R30^\circ$ O-rich surface*

Figure 6 shows valence band photoemission spectra of the  $V_2O_3(0001)(\sqrt{3} \times \sqrt{3})R30^\circ$  surface recorded at 300 and 100 K with photon energies  $h\nu = 110$  eV (curves (a), (b)) and  $h\nu = 517$  eV (curves (c)). The spectra of figures 6(a) and (b) have been taken with  $h\nu = 110$  eV at normal and grazing emission geometry, respectively. There is some shift of the spectral weight away from  $E_F$  upon cooling, but this effect is less pronounced on the  $(\sqrt{3} \times \sqrt{3})R30^\circ$  surface than on the  $(1 \times 1)$  surface. This is clearly apparent from figure 6(c), where the grazing emission 100 K valence band spectra of the  $(1 \times 1)$   $V=O$  surface and the  $(\sqrt{3} \times \sqrt{3})R30^\circ$  surface are compared. The O-rich  $(\sqrt{3} \times \sqrt{3})R30^\circ$  surface has significantly more spectral weight in the region from  $E_F$  to 0.75 eV below  $E_F$  than the  $(1 \times 1)$  surface (figure 6(c)) and thus appears to be more ‘metallic’ at 100 K. This is corroborated by the HREELS measurements



**Figure 6.** V 3d valence band photoemission spectra of the  $\text{V}_2\text{O}_3(0001)$  ( $\sqrt{3} \times \sqrt{3}$ )R30° surface recorded at 300 and 100 K in normal emission (a) and grazing emission (b) geometry,  $h\nu = 110$  eV. Panel (c) compares the V 3d spectra of the (1 × 1)-V=O and the ( $\sqrt{3} \times \sqrt{3}$ )R30° surface recorded at 100 K,  $h\nu = 517$  eV. The spectra have been normalized as in figure 4.

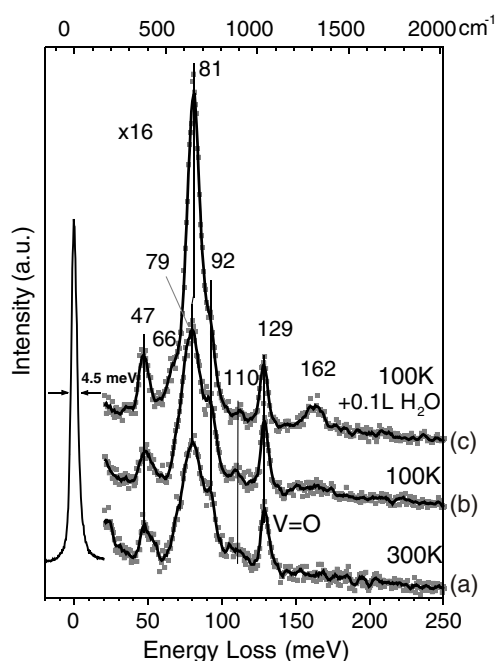


**Figure 7.** HREELS spectra of the  $(\sqrt{3} \times \sqrt{3})R30^\circ$  surface recorded at 300 K (a) and 100 K (b). Curve (c) shows the HREELS spectrum of the  $(\sqrt{3} \times \sqrt{3})R30^\circ$  surface at 100 K after exposure to 0.1 L of  $H_2O$ .

of figure 7. The loss curves of the  $(\sqrt{3} \times \sqrt{3})R30^\circ$  surface recorded at 300 K (figure 7(a)) and 100 K (figure 7(b)) are virtually identical; the changes seen in the HREELS on the  $(1 \times 1)$  surface as a result of the MIT (figure 5) are not reproduced on the  $(\sqrt{3} \times \sqrt{3})R30^\circ$  surface. Taken together, these results suggest that the MIT occurring in the bulk of the  $V_2O_3$  film is effectively screened at the surface by the local rearrangement of subsurface layers on the  $(\sqrt{3} \times \sqrt{3})R30^\circ$  surface. According to the DFT calculations [14], the removal of vanadyl groups to form the  $(\sqrt{3} \times \sqrt{3})R30^\circ$  reconstruction leads locally to the formation of a  $-V_2O_3-V-O_3V_3O_3$  stacking sequence, i.e. to a trilayer structure with a formal  $VO_2$  stoichiometry on top of a single V layer. The first bulk-type  $O_3$  layer is thus five layers below the diluted  $V=O$  containing  $(\sqrt{3} \times \sqrt{3})R30^\circ$  surface layer. The electronic structure of the  $O_3V_3O_3$  trilayer is quite different from the ideal  $O_3$  bulk termination with an average number of conduction band electrons of one per V atom in the former, as expected from the formal  $IV+$  oxidation state. The present photoemission and HREELS spectra thus indicate that the MIT in the  $V_2O_3$  bulk film is less effectively communicated to the experimental probes through the subsurface  $VO_2$  trilayer of the  $(\sqrt{3} \times \sqrt{3})R30^\circ$  surface than through the vanadyl surface layer on the  $(1 \times 1)$  surface.

An interesting effect has been observed on the  $(\sqrt{3} \times \sqrt{3})R30^\circ$  reconstruction upon adsorption of trace amounts of molecular water at 100 K. Figure 7(c) shows the HREELS spectrum of a  $V_2O_3(0001)(\sqrt{3} \times \sqrt{3})R30^\circ$  surface, which had been exposed to approximately one-tenth of a monolayer of  $H_2O$  (0.06 L; 1 L (Langmuir) =  $1 \times 10^{-6}$  Torr  $\times$  s) at 100 K. The 79 meV phonon is shifted to 81 meV with dramatically increased intensity after the adsorption of water, and a weak shoulder has developed at around 66 meV. This resembles the fingerprint of the MIT of  $V_2O_3$  in HREELS as observed on the  $(1 \times 1)$  surface in figure 5, suggesting that

the MIT becomes transmitted through the  $(\sqrt{3} \times \sqrt{3})R30^\circ$  reconstruction by the ‘doping’ of the surface with adsorbed  $H_2O$ . This effect of water is reversible and the MIT related HREELS spectrum (figure 7(c)) returns to the one without MIT signature (figure 7(b)) after desorption of the molecular water at  $T \approx 200$  K. Note that the molecular vibrations of adsorbed water molecules at low coverages cannot be discerned in the HREELS spectra, because the strong oxide phonon peaks dominate the spectra.

We propose the following scenario to rationalize these water induced effects on the  $(\sqrt{3} \times \sqrt{3})R30^\circ$  HREELS spectrum. At very low coverages it is plausible that the  $H_2O$  molecules adsorb at surface sites, where the vanadyl groups are missing in the  $(\sqrt{3} \times \sqrt{3})R30^\circ$  unit cells. It is at these sites that the  $VO_2$  trilayer reconstruction is formed by local relaxation of the surface as a response to the missing vanadyls. We conjecture that the electrostatic potential of the  $H_2O$  molecules adsorbed at these sites reverts to this reconstruction, leading to a more bulk-like  $-V_2-O_3$  termination below the adsorbed water molecules. The observation of the MIT in the  $V_2O_3$  bulk with surface sensitive techniques may then be less effectively screened.

## 5. Summary

The effect of different surface terminations of  $V_2O_3(0001)$  thin-film surfaces, which have been grown epitaxially on Rh(111) substrates, on the metal–insulator transition of  $V_2O_3$  has been investigated by valence band photoemission spectroscopy and high-resolution electron energy loss spectroscopy. We find that the surface reconstructions do have a strong effect on the observation of the MIT: the reconstructed surface layers do not take part in the MIT. This is an additional effect to the intrinsic surface effect of increased correlation at the surface due to the reduced coordination numbers of surface atoms.

The most stable surface of  $V_2O_3(0001)$  at intermediate chemical potentials of oxygen (as typical for ultrahigh vacuum experiments) is a  $(1 \times 1)$  surface terminated with vanadyl  $V=O$  groups, which are arranged in a hexagonal (0001) bulk lattice array. The MIT through this surface is evidenced by the changes in the spectral weight of the electronic density of states close to the Fermi level in the valence band photoemission spectra and by the modifications of the phonon spectra in HREELS upon cooling the films from 300 to 100 K. Both experiments and electronic structure DFT calculations suggest that the vanadyl surface layer does not itself support the MIT, but that the MIT of the  $V_2O_3$  in the bulk can be picked up by the surface sensitive experimental probes *through* the vanadyl surface layer. On the oxygen-rich  $V_2O_3(0001)(\sqrt{3} \times \sqrt{3})R30^\circ$  surface termination, which is characterized by a  $(\sqrt{3} \times \sqrt{3})R30^\circ$  array of missing vanadyl groups and a local surface reconstruction involving four layers below the topmost  $(\sqrt{3} \times \sqrt{3})R30^\circ$  surface layer, the MIT is more effectively screened at the surface by the reconstructed subsurface layers. Doping the  $(\sqrt{3} \times \sqrt{3})R30^\circ$  surface with small amounts of adsorbed water molecules restores reversibly the MIT spectral fingerprints in HREELS. It is speculated that the adsorbed water molecules relax the local deep surface reconstructions, restoring a more bulk-like subsurface situation, from which the MIT can be communicated again through the surface layers. Finally, when measuring the MIT effect with surface sensitive methods the exact nature of the surface must be considered.

## Acknowledgments

This work has been supported by the Austrian Science Funds through the Joint Research Programme ‘Nanoscience on Surfaces’. The synchrotron radiation measurements at MAX-Lab have been supported by the EU-TMR programme under contract ERB FMGE CT98 0124. The support of the MAX-Lab staff is gratefully acknowledged.

## References

- [1] Foex M 1946 *C. R. Acad. Sci.* **223** 1126
- [2] McWhan D B, Rice T M and Remeika J P 1969 *Phys. Rev. Lett.* **23** 1384
- [3] Park J-H *et al* 2000 *Phys. Rev. B* **61** 11506
- [4] Paolasini L *et al* 1999 *Phys. Rev. Lett.* **82** 4719
- [5] Di Matteo S, Perkins N A and Natoli C R 2002 *Phys. Rev. B* **65** 054413
- [6] Mo S-K *et al* 2003 *Phys. Rev. Lett.* **90** 186403
- [7] Maiti K, Mahadevan P and Sarma D D 1998 *Phys. Rev. Lett.* **80** 2885
- [8] Schwieger S, Potthoff M and Nolting W 2003 *Phys. Rev. B* **67** 165408
- [9] Preisinger M, Moosburger-Will J, Klemm M, Klimm S and Horn S 2004 *Phys. Rev. B* **69** 075423
- [10] Schuler H, Klimm S, Weissmann G, Renner C and Horn S 1997 *Thin Solid Films* **299** 119
- [11] Luo Q, Guo Q and Wang E G 2004 *Appl. Phys. Lett.* **84** 2337
- [12] Sass B, Tusche C, Felsch W, Quaas N, Weissmann A and Wenderoth M 2004 *J. Phys.: Condens. Matter* **16** 77
- [13] Schoiswohl J, Sock M, Surnev S, Ramsey M G, Netzer F P, Kresse G and Andersen J N 2004 *Surf. Sci.* **55** 101
- [14] Kresse G, Surnev S, Schoiswohl J and Netzer F P 2004 *Surf. Sci.* **55** 118
- [15] Poelman H, Vennik J and Dalmai G 1987 *J. Electron Spectrosc. Relat. Phenom.* **44** 251
- [16] Kardinal I, Netzer F P and Ramsey M G 1997 *Surf. Sci.* **376** 229
- [17] Mo S-K *et al* 2004 *Phys. Rev. Lett.* **93** 076404
- [18] Guo Q, Kim D Y, Street S C and Goodman D W 1999 *J. Vac. Sci. Technol. A* **17** 1887
- [19] Dupuis A-C, Abu Haija M, Richter B, Kuhlbeck H and Freund H-J 2003 *Surf. Sci.* **539** 99